Full Papers

CFD Simulations of a Bubble Column Operating in the Homogeneous and Heterogeneous Flow Regimes

By *J. M. van Baten* and *R. Krishna**

Bubble columns are operated either in the homogeneous or heterogeneous flow regime. In the homogeneous flow regime, the bubbles are nearly uniform in size and shape. In the heterogeneous flow regime, a distribution of bubble sizes exists. In this paper, a CFD model is developed to describe the hydrodynamics of bubble columns operating in either of the two flow regimes. The heterogeneous flow regime is assumed to consist of two bubble classes: "small" and "large" bubbles. For the air-water system, appropriate drag relations are suggested for these two bubble classes. Interactions between both bubble populations and the liquid are taken into account in terms of momentum exchange, or drag-, coefficients, which differ for the "small" and "large" bubbles. Direct interactions between the large and small bubble phases are ignored. The turbulence in the liquid phase is described using the k-ε model. For a 0.1 m diameter column operating with the air-water system, CFD simulations have been carried out for superficial gas velocities, U, in the range 0.006–0.08 m/s, spanning both regimes. These simulations reveal some of the characteristic features of homogeneous and heterogeneous flow regimes, and of regime transition.

1 Introduction

When a column filled with a liquid is sparged with gas, the bed of liquid begins to expand as soon as gas is introduced. As the gas velocity is increased, the gas holdup ε increases almost linearly with the superficial gas velocity, U, provided the value of U stays below a certain value U_{trans}. This regime of operation of a bubble column is called the *homogeneous bubbly flow regime*. The bubble size distribution is narrow and a roughly uniform bubble size, generally in the range 1–7 mm, is found. When the superficial gas velocity U reaches the value U_{trans}, coalescence of the bubbles takes place to produce the first fast-rising "large" bubble. The appearance of the first large bubble changes the hydrodynamic picture dramatically. The hydrodynamic picture in a gas-liquid system for velocities exceeding U_{trans} is commonly referred to as the *heterogeneous* or *churn-turbulent flow regime* [1]. In the heterogeneous regime, small bubbles combine in clusters to form large bubbles in the size range 20–70 mm [2]. These large bubbles travel up through the column at high velocities (in the range 1–2 m/s), in a more or less plug flow manner [3]. These large bubbles have the effect of churning up the liquid phase and because of their high rise velocities they account for a major fraction of the gas throughput [4]. Small bubbles, which coexist with large bubbles in the churn-turbulent regime, are "entrained" in the liquid phase and, as a good approximation, have the same back-mixing characteristics of the liquid phase [5]. The two regimes are portrayed in Fig. 1 for operation of a bubble column of 0.1 m diameter with the air-water system.

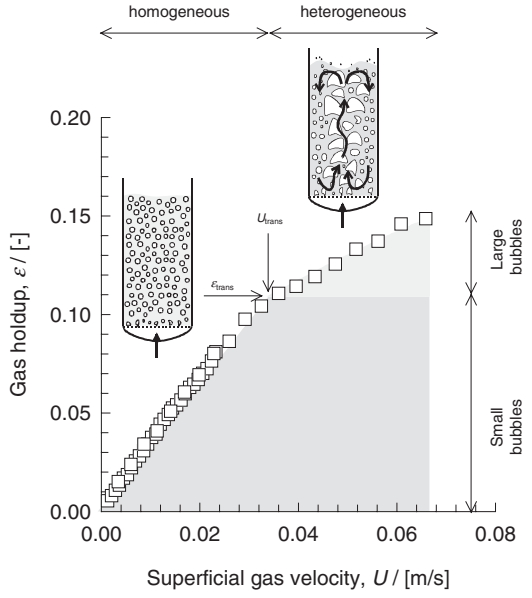

Figure 1. Experimental data on gas holdup in a 0.1 m diameter bubble column operating with the air-water system spanning both the homogeneous and heterogeneous flow regimes.

Several recent publications have established the potential of Computational Fluid Dynamics (CFD) for describing the hydrodynamics of bubble columns [6–17]. These CFD models are developed for either the homogeneous [8–11] or heterogeneous [12–17] flow regimes. The first major objective of the present communication is to develop a CFD model to describe both regimes, including regime transition. The second objective is to examine the extent to which CFD models are able to describe quantitatively the variation of ε with U in both flow regimes. This study helps to underline the distinguishing characteristics of both regimes.

[*] J. M. van Baten, R. Krishna (author to whom correspondence should be addressed, e-mail: krishna@science.uva.nl), Department of Chemical Engineering, University of Amsterdam, Nieuwe Achtergracht 166, 1018 WV Amsterdam, The Netherlands.

  0930-7516/02/1111-1081 $ 17.50+.50/0

2 Development of CFD Model

Our approach for modeling purposes is to assume that in the heterogeneous flow regime we have two distinct bubble classes: "small" and "large"; see Fig. 2. The small bubbles are either spherical or ellipsoidal in shape depending on the physical properties of the liquid [18]. The large bubbles fall into the spherical cap regime. In conformity with the model of Krishna and Ellenberger [3], we assume that the superficial gas velocity through the small bubble phase corresponds to that at the regime transition point, U_{trans}. The transition velocity can be estimated using the Reilly *et al.* [19] correlation, or can be provided as model input.

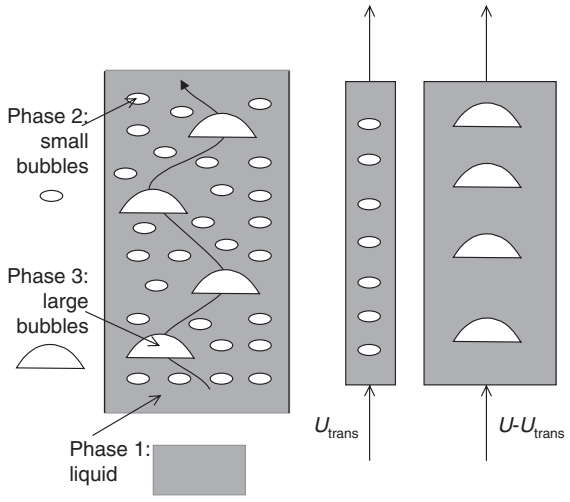

Figure 2. Model for bubble columns operating in the heterogeneous flow regime.

For each of the three phases shown in Fig. 2 the volume-averaged mass and momentum conservation equations in the Eulerian framework are given by[1)]:

$$\frac{\partial(\varepsilon_k\rho_k)}{\partial t} + \nabla\cdot(\rho_k\varepsilon_k\mathbf{u}_k) = 0 \tag{1}$$

$$\frac{\partial(\rho_k\varepsilon_k\mathbf{u}_k)}{\partial t} + \nabla\cdot\left(\rho_k\varepsilon_k\mathbf{u}_k\mathbf{u}_k - \mu_k\varepsilon_k\left(\nabla\mathbf{u}_k + (\nabla\mathbf{u}_k)^{\mathrm{T}}\right)\right) = -\varepsilon_k\nabla p + \mathbf{M}_{kl} + \rho_k\mathrm{g} \tag{2}$$

where ρ_k, $\mathbf{u}_k$, ε_k and μ_k represent, respectively, the macroscopic density, velocity, volume fraction and viscosity of the kth phase, p is the pressure, $\mathbf{M}_{kl}$, the interphase momentum exchange between phase k and phase l and $\mathbf{g}$ is the gravitational acceleration.

The momentum exchange between either bubble phase (subscript b) and liquid phase (subscript L) phases is given by

$$\mathrm{M}_{L,b} = \frac{3}{4}\rho_L\frac{\varepsilon_b}{d_b}C_D(\mathbf{u}_b - \mathbf{u}_L)|\mathbf{u}_b - \mathbf{u}_L| \tag{3}$$

The liquid phase exchanges momentum with both the "small" and "large" bubble phases. No interchange between the "small" and "large" bubble phases have been included in the present model and each of the dispersed bubble phases exchanges momentum only with the liquid phase. The interphase drag coefficient is calculated from equation

$$C_D = \frac{4}{3}\frac{\rho_L-\rho_G}{\rho_L}gd_b\frac{1}{V_b^2} \tag{4}$$

where V_{b} is the rise velocity of the appropriate bubble population. We have only included the drag force contribution to $\mathbf{M}_{\mathrm{L,b}}$, in keeping with the works of Sanyal *et al.* [9] and Sokolichin and Eigenberger [10]. The added mass and lift forces have been ignored in the present analysis.

For the continuous, liquid, phase, the turbulent contribution to the stress tensor is evaluated by means of the k-ε model, using standard single-phase parameters $C_\mu = 0.09$, $C_{1\varepsilon} = 1.44$, $C_{2\varepsilon} = 1.92$, $\sigma_{\mathrm{k}} = 1$ and $\sigma_\varepsilon = 1.3$. No turbulence model is used for calculating the velocity fields inside the dispersed "small" and "large" bubble phases.

For the small bubbles the interphase drag coefficient is calculated from [18]:

$$C_D = \frac{2}{3}\sqrt{\mathrm{E\ddot{o}}} \tag{5}$$

with

$$E\ddot{o} = \frac{g(\rho_L-\rho_G)d_b^2}{\sigma} \tag{6}$$

where d_{b} is the equivalent diameter of the bubbles. For a single bubble rising in a quiescent liquid, the rise velocity V_{b0} can be calculated from the drag coefficient:

$$V_{b0} = \sqrt{\frac{(\rho_L-\rho_G)g}{\frac{3C_D}{4d_b}\rho_L}} \tag{7}$$

The calculations of the single bubble rise velocity V_{b0} using Eqs. (5)–(7) compare very well with the rise velocity of single air bubbles in water [20]; see Fig. 3(a). We note that the rise velocity is practically independent of the bubble size in the 3–8 mm range. For the simulations reported here, we choose a small bubble diameter $d_{\mathrm{b}} = 5$ mm.

For values of Eö > 40 (for air-water system, this corresponds to bubble sizes larger than 17 mm), bubbles assume a spherical cap shape. The rise velocity of spherical cap bubbles is given by the classic Davies and Taylor [21] relationship:

$$V_{b0} = \sqrt{gd_b/2} = 0.71\sqrt{gd_b} \tag{8}$$

The calculations of the single bubble rise velocity V_{b0} using Eq. (8) compare very well with the rise velocity of single air bubbles in water [20] in the 17–60 mm size range; see Fig. 3 (b).

The drag coefficient for these large bubbles is given by

$$C_D = \frac{8}{3} \tag{9}$$

In the simulations reported below, a large bubble diameter of 20 mm was used.

1) List of symbols at the end of the paper.

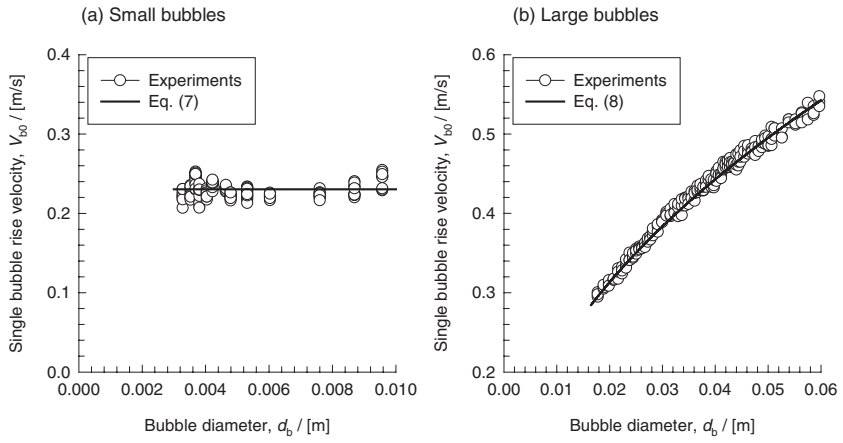

Figure 3. Experimental data on single bubble rise velocity as a function of bubble diameter [20], compared with predictions of the drag model adopted in this work for (a) small bubbles and (b) large bubbles.

A commercial CFD package CFX, versions 4.2 and 4.4, of AEA Technology, Harwell, UK, was used to solve the equations of continuity and momentum. This package is a finite volume solver, using body-fitted grids. The grids are nonstaggered and all variables are evaluated at the cell centers. An improved version of the Rhie-Chow algorithm [22] is used to calculate the velocity at the cell faces. The pressure-velocity coupling is obtained using the SIMPLEC algorithm [23]. For the convective terms in Eqs. (1) and (2), hybrid differencing was used. A fully implicit backward differencing scheme was used for the time integration.

Simulations were carried out for a 0.1 m diameter bubble column with the air-water system, operating at superficial gas velocities in the range $U = 0.006$ to 0.08 m/s. From the Reilly *et al.* correlation [19] it was determined that the superficial gas velocity at the regime transition point for air-water is $U_{trans} = 0.034$ m/s; this is also the value of the regime transition velocity for the experimental data shown in Fig. 1. For air-water operation at $U < 0.034$ m/s, homogeneous bubbly flow regime was taken to prevail. Therefore, only two phases—small bubbles and liquid—are present. For churn-turbulent operation at $U > 0.034$ m/s, the complete three-phase model was invoked. Following the model of Krishna and Ellenberger [3], we assume that in the churn-turbulent flow regime the superficial gas velocity through the small bubble phase is $U_{trans} = 0.034$ m/s (see Fig. 2). The remainder of the gas ($U–U_{trans}$) was taken to rise up the column in the form of large bubbles. This implies that at the distributor the "large" bubbles constitute a fraction $(U–U_{trans})/U$ of the total incoming volumetric flow, whereas the "small" bubbles constitute a fraction (U_{trans}/U) of the total incoming flow.

The simulations were carried out using axi-symmetric 2-D grids. The grid details are shown in Fig. 4; the total number of grid cells is 1500. The small bubbles were injected at the inner 12 of 15 cells in the bottom patch. The large bubbles were injected at the inner 9 of 15 cells of the bottom patch. A pressure boundary condition was applied to the top of the column. A standard no-slip boundary condition was applied at all walls. The time stepping strategy used in all simulations was 100 steps at 5×10^{-5} s, 100 steps at 1×10^{-4} s, 100 steps at 5×10^{-4} s, 100 steps at 1×10^{-3} s, 200 steps at 3×10^{-3} s, 1400 steps at 5×10^{-3} s, and the remaining steps until steady state is achieved at 1×10^{-2} s. Steady state was indicated by a situation in which all of the variables remained constant.

The 2-D simulations were carried out on Silicon Graphics Power Indigo workstations with 75 MHz R8000 processors, a Silicon Graphics O2 workstation with a 150 MHz R10000 processor and a Windows NT PC with a single Pentium Celeron processor running at 500 MHz. Each simulation was completed in about a day.

Further computational details of the model and simulations, along with animations, are available on our web site: http://ct-cr4.chem.uva.nl/regimes/.

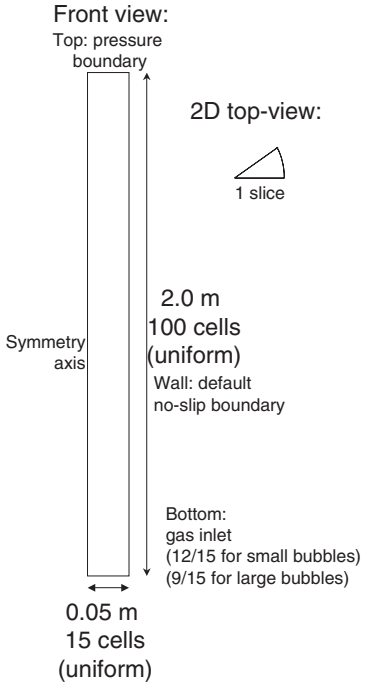

Figure 4. Computational grid details.

3 Simulation Results

A typical transience of the gas and liquid velocities, at the center of the column, are shown in Fig. 5 for operation at U = 0.02 and 0.05 m/s. Steady state is reached within about 4000 time steps. The steady-state values of all the hydrodynamic parameters were determined at a position 1 m above the distributor and reported below.

The radial distributions of gas holdup and liquid velocities, at steady state, for operation in the homogeneous flow regime ($U \leq 0.034$ m/s) are shown in Fig. 6. There is substantial downflow of liquid near the walls; this downflow velocity increases with U. With increasing U, the gas holdup profiles lose their plug flow character in increasing measure, and assume a parabolic shape.

The radial distributions of total gas holdup and liquid velocities, at steady state, for operation in the heterogeneous flow regime ($U > 0.034$ m/s) are shown in Fig. 7. With increasing gas velocity, the gas bubbles tend to concentrate more and more in the central core of the column. This concentration of bubbles in the central core causes a substantial increase in the liquid circulations, evidenced by the increasingly large downward flow near the walls.

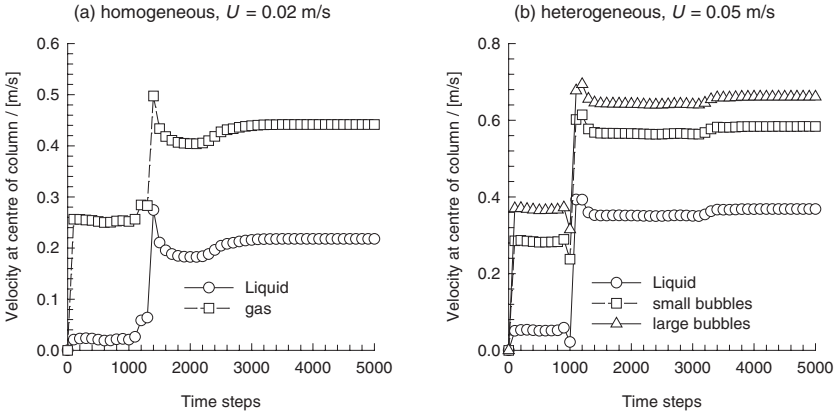

Figure 5. Transient approach to steady state in the bubble column. Simulation results for (a) U = 0.020 m/s and (b) U = 0.05 m/s. Values monitored at a height of 1 m above the distributor. Animations can be viewed on the web-site: http://ct-cr4.chem.uva.nl/regimes/.

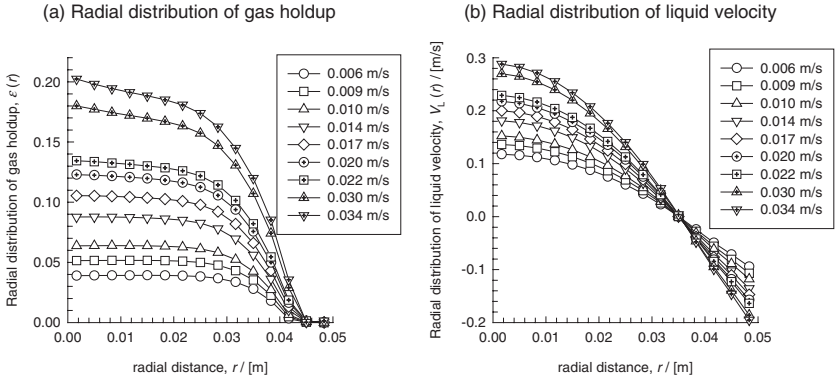

Figure 6. Radial distribution of gas holdup $\varepsilon_G(r)$ and liquid velocity $V_L(r)$ for varying superficial gas velocities U in the homogeneous flow regime. Values monitored at a height of 1 m above the distributor.

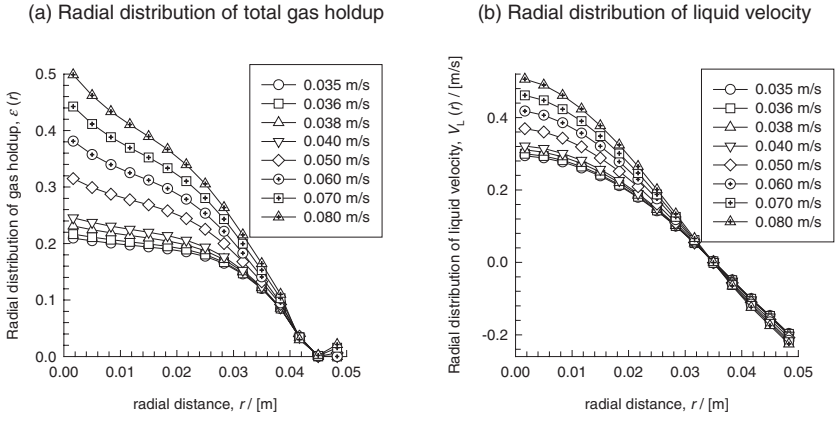

Figure 7. Radial distribution of gas holdup $\varepsilon_G(r)$ and liquid velocity $V_L(r)$ for varying superficial gas velocities U in the heterogeneous flow regime. Values monitored at a height of 1 m above the distributor.

The radial distribution of the *fraction* of the total gas holdup that is present as (a) small and (b) large bubbles is shown in Fig. 8. With increasing superficial gas velocity the fraction of large bubbles increases; this increase takes place almost exclusively in the central core of the column. In the heterogeneous flow regime the small bubbles tend to concentrate near the peripheral, wall-, regions.

The cross-sectional area averaged values of the gas holdup and the center-line liquid velocities are shown in Figs. 9(a) and (b). Also plotted in Fig. 9(a) are the values of the small bubble holdup. In the heterogeneous flow regime, the small bubble holdup attains a constant value, equal to the holdup at the regime transition point, ε_{trans}. This assumption is basic to the model of Krishna and Ellenberger [3] for prediction of the estimation of the total gas holdup in the heterogeneous flow regime. We also note a sharp change in the slope of the ε vs. U curve at $U = U_{trans}$; this is consistent with experimental data obtained in a 0.1 m diameter (also in Fig. 9(a)). For the center-line liquid velocity, $V_L(0)$, there is no sharp change in the values at the regime transition point.

4 Conclusions

We have developed a CFD model to describe the hydrodynamics of an air-water bubble column operating in both homogeneous and heterogeneous flow regimes. In the heterogeneous flow regime, the large bubbles are found to concentrate in the central core of the bubble column, whereas the small bubbles are distributed throughout the column.

The small bubble holdup is practically constant in the heterogeneous flow regime and its value corresponds to that at the regime transition point. Our CFD simulations verify this basic assumption of the Krishna-Ellenberger [3] model.

Acknowledgement

The Netherlands Organisation for Scientific Research (NWO) is gratefully acknowledged for providing financial assistance in the form of a "programmasubsidie" for development of novel concepts in reactive separations technology.

Received: May 6, 2002 [CET 1601]

Symbols used

C_D	[–]	drag coefficient, dimensionless
d_b	[m]	diameter of bubble
D_T	[m]	column diameter
Eö	[–]	Eötvös number, $g(\rho_L - \rho_g)d_b^2/\sigma$

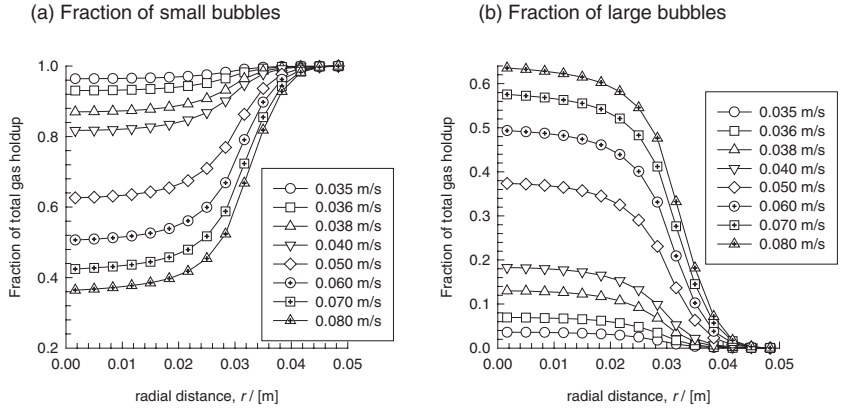

Figure 8. Radial distribution of the fraction of total gas holdup that is present as (a) small bubbles, and (b) large bubbles for varying superficial gas velocities U in the heterogeneous flow regime. Values monitored at a height of 1 m above the distributor.

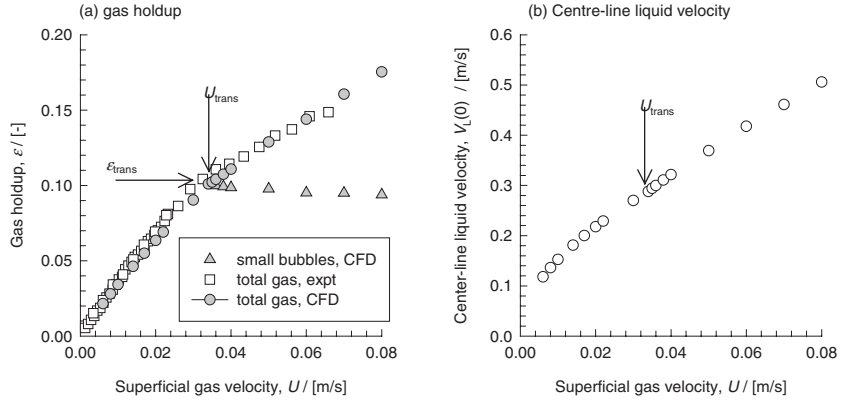

Figure 9. (a) Cross-sectional area averaged gas holdup as a function of the superficial gas velocity. Both the total gas holdup and the small bubble holdup are shown. (b) Center-line liquid velocity as a function of the superficial gas velocity. Also plotted is the total gas holdup data for air-water system in a 0.1 m diameter column.

g	[m s^{-2}]	gravitational acceleration, 9.81 m s^{-2}
$\boldsymbol{g}$	[m s^{-2}]	gravitational vector
$\mathbf{M}$	[N/m^3]	interphase momentum exchange term
p	[Pa]	system pressure
r	[m]	radial coordinate
t	[s]	time
$\mathbf{u}$	[m/s]	velocity vector
U	[m s^{-1}]	superficial gas velocity in the riser
$V_L(r)$	[m s^{-1}]	radial distribution of liquid velocity
$V_L(0)$	[m s^{-1}]	center-line liquid velocity
V_b	[m s^{-1}]	bubble rise velocity
V_{b0}	[m s^{-1}]	single bubble rise velocity

Greek symbols

ε	[–]	total gas holdup, dimensionless
μ	[Pa s]	viscosity of fluid phase
ρ	[kg m^{-3}]	density of phase
σ	[N m^{-1}]	surface tension of liquid phase

Subscripts

b	referring to bubbles
L	referring to liquid
T	tower or column
k,l	referring to phase k and l respectively

References

[1] W. D. Deckwer, *Bubble Column Reactors, John Wiley & Sons, New York* **1992.**

[2] J. W. A. de Swart, R. E. van Vliet, R. Krishna, Size, Structure and Dynamics of "Large" Bubbles in a 2-D Slurry Bubble Column, *Chem. Eng. Sci.* **1996**, *51*, 4619.

[3] R. Krishna, J. Ellenberger, Gas Hold-up in Bubble Column Reactors Operating in the Churn-Turbulent Flow Regime, *AIChE J.* **1996**, *42*, 2627.

[4] R. Krishna, J. Ellenberger, S. T. Sie, Reactor Development for Conversion of Natural Gas to Liquid Fuels: A Scale-up Strategy Relying on Hydrodynamic Analogies, *Chem. Eng. Sci*. **1996**, *51*, 2041.

[5] R. Krishna, S. T. Sie, Design and Scale-up of the Fischer-Tropsch Bubble Column Slurry Reactor, *Fuel Process. Technol.* **2000**, *64*, 73.

[6] H. A. Jakobsen, B, H: Sannæs, S. Grevskott, H. F.Svendsen, Modeling of Bubble-Driven Vertical Flows, *Ind. Eng. Chem. Res.* **1997**, *36*, 4052.

[7] J. B. Joshi, Computational Flow Modelling and Design of Bubble Column Reactors, *Chem. Eng. Sci.* **2001**, *56*, 5893.

[8] Y. Pan, M. P. Dudukovic, M. Chang, Numerical Investigation of Gas-Driven Flow in 2-D Bubble Columns, *AIChE J.* **2000**, *46*, 434.

[9] J. Sanyal, S: Vasquez, S. Roy, M. P. Dudukovic, Numerical Simulation of Gas-Liquid Dynamics in Cylindrical Bubble Column Reactors, *Chem. Eng. Sci*. **1999**, *54*, 5071

[10] A. Sokolichin, G. Eigenberger, Applicability of the Standard-Turbulence Model to the Dynamic Simulation of Bubble Columns: Part I., Detailed Numerical Simulations, *Chem. Eng. Sci.* **1999**, *54*, 2273.

[11] R. Krishna, J. M. van Baten, M. I. Urseanu, Scale Effects on the Hydrodynamics of Bubble Columns Operating in the Homogeneous Flow Regime, *Chem. Eng. Technol.* **2001**, *24*, 451.

[12] R. Krishna, M. I. Urseanu, J. M. van Baten, J. Ellenberger, Influence of Scale on the Hydrodynamics of Bubble Columns Operating in the Churn-Turbulent Regime: Experiments vs Eulerian Simulations, *Chem. Eng. Sci.* **1999**, *54*, 4903.

[13] R. Krishna, J. M. van Baten, M. I. Urseanu, Three-Phase Eulerian Simulations of Bubble Column Reactors Operating in the Churn-Turbulent Flow Regime: A Scale-up Strategy, *Chem. Eng. Sci*. **2000**, *55*, 3275.

[14] R. Krishna, J. M. Van Baten, Eulerian Simulation of Bubble Columns Operated at Elevated Pressures in the Churn-Turbulent Regime, *Chem. Eng. Sci.* **2001**, *56*, 6249.

[15] J. M: van Baten, R. Krishna, Eulerian Simulations for Determination of the Axial Dispersion of Liquid and Gas Phases in Bubble Columns Operating in the Churn-Turbulent Regime, *Chem. Eng. Sci.* **2001**, *56*, 503.

[16] R. Krishna, J. M. van Baten, Scaling up Bubble Column Reactors with the Aid of CFD, *Chem. Eng. Res. Des., Trans. Inst. Chem. Eng*. **2001**, *79*, 283.

[17] R. Krishna, J. M. van Baten, M. I. Urseanu, J. Ellenberger, Design and Scale-up of the Bubble Column Slurry Reactor for Fischer-Tropsch Synthesis, *Chem. Eng. Sci.* **2001**, *56*, 537.

[18] R. Clift, J. R. Grace, M. E. Weber, *Bubbles, Drops and Particles*, Academic Press, San Diego **1978**.

[19] I. G. Reilly, D. S. Scott, T. J. W. de Bruijn, D. MacIntyre, The Role of Gas-phase Momentum in Determining Gas Holdup and Hydrodynamic Flow Regimes in Bubble Column Operations, *Can. J. Chem. Eng.* **1994**, *72*, 3.

[20] R. Krishna, M. I: Urseanu, J. M. van Baten, J. Ellenberger, Wall Effects on the Rise of Single Gas Bubbles in Liquids, *Int. Comm. Heat Mass Trans.* **1999**, *26,* 781.

[21] R. M. Davies, G. I. Taylor, The Mechanics of Large Bubbles Rising through Extended Liquids and through Liquids in Tubes, *Proc. Roy. Soc. London*, A200, **1950**, 375.

[22] C. M. Rhie, W. L. Chow, Numerical Study of the Turbulent Flow past an Airfoil with Trailing Edge Separation, *AIAA J.* **1983**, *21*, 1525.

[23] J. van Doormal, G. D. Raithby, Enhancement of the SIMPLE Method for Predicting Incompressible Flows, *Numer. Heat Trans.* **1984**, *7*, 147.

